

Classification of OH Bonds and Infrared Spectra of the Topology-Distinct Protonated Water Clusters $\text{H}_3\text{O}^+(\text{H}_2\text{O})_{n-1}$ ($n \leq 7$)

Maihemutijiang Jieli and Misako Aida*

Center for Quantum Life Sciences and Department of Chemistry, Graduate School of Science, Hiroshima University, Kagamiyama, Higashi-Hiroshima, 739-8526 Japan

Received: December 6, 2008; Revised Manuscript Received: December 21, 2008

Rooted digraphs are used to represent the features of a protonated water (PW) cluster, and we obtain all possible topology-distinct patterns corresponding to PW clusters containing up to seven water molecules. From close investigation of the structural patterns obtained, several restrictions that should be satisfied in the stable structures of PW clusters are found. The generated hydrogen bond (HB) matrices of the restrictive rooted digraph are used as the theoretical framework to obtain all of the local minima on the potential energy surfaces of those PW clusters by the use of ab initio MO and DFT methods. For PW pentamers, hexamers, and heptamers, some new local minimum structures were found that were not previously obtained. We classify all of the O–H bonds in PW clusters up to heptamer into nine types according to the difference in the hydrogen bonding pattern; each type is accompanied by a specific range of stretching frequency. The ranges of stretching frequencies of different types of O–H in PW clusters are systematically classified.

Introduction

Protonated water (PW) clusters are common in nature and play important roles in many fields of science including atmospheric chemistry, solution chemistry, and biological chemistry. In particular, they are the most abundant cluster ions in the stratosphere and actively participate in a variety of atmospheric nucleation and reactions associated with water.^{1,2} It is known³ that the presence of excess protons has a profound influence on the phase transition of small water aggregates under atmospheric conditions. They are also found in restricted spaces and cavities of proteins and biomolecules.⁴

There are a lot of stable structures in PW clusters with various arrangements of the constituent water molecules. The number of available structures (the hydrogen bonding patterns) plays an important role in thermodynamic properties of PW clusters. The number of local minima rapidly increases with the cluster size.

Concerning PW clusters, there have been many previous experimental studies^{5–11} to measure the infrared spectra and theoretical studies^{12–31,34,45–48,50–53} in various aspects using different methods and levels of theory. But neither of those studies has been devoted to elucidating all of the possible structures and neither has generated IR spectra of all different patterns of stable PW clusters systematically. It is not trivial to present all of the possible structures or to claim that a structure is indeed the global minimum.

A graph represents the connection between the constituents, which is related to the topology of a given molecule or molecular cluster. Graph theory has been used successfully and extensively to represent various properties of molecules, such as thermodynamic properties of alkanes³² and π -electron energies of aromatic hydrocarbons.³³ A graph theoretical technique has been introduced to generate neutral and PW cubes and dodecahedral clusters for $(\text{H}_2\text{O})_8$, $(\text{H}_2\text{O})_{20}$, $\text{H}^+(\text{H}_2\text{O})_8$ and $\text{H}^+(\text{H}_2\text{O})_{20}$.³⁴

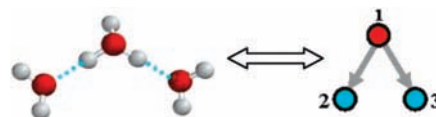


Figure 1. Structure of PW cluster and the corresponding rooted digraph.

The hydrogen bond (HB) can form long-lived structures for neutral and protonated water clusters. The important feature of the HB is that it possesses direction; in an HB, a hydrogen atom is donated to an acceptor (oxygen atom). The direction can be indicated by an arrow. In our previous study, we presented a graph theoretical procedure for generating all of the topology-distinct structures of neutral water clusters^{35,36} and PW clusters³⁷ by means of a digraph (or a rooted digraph) corresponding to the set of arrows (Figure 1).

In this Article, all possible topology-distinct local minima on the potential energy surfaces of $\text{H}_3\text{O}^+(\text{H}_2\text{O})_{n-1}$ ($n = 4$ to 6) are given. The harmonic vibrational frequencies and their infrared intensities at MP2(full) level of theory and aug-cc-pVDZ basis set are calculated. The number of local minima might vary when a different level of theory or any potential function is used for the calculation of the potential energy surface. The important point is that we know all of the possible topology-distinct HB patterns of the PW cluster after the enumeration; that is, we know that there cannot be other patterns. Furthermore, the characteristic IR harmonic vibrational frequencies of different HB types of PW clusters are systematically demonstrated.

Theory and Computational Details

A graph is a set of vertices and edges, and a graph corresponding to a PW cluster is a kind of rooted graph because a PW is distinguished from other water molecules in the PW cluster. For a rooted graph with n vertices, the adjacency matrix, \mathbf{A} , is the n th-order square matrix, whose element, a_{ij} , is equal to 1 for a pair of vertices i and j that are connected by an edge

* Corresponding author. Tel: +81-82-424-7412. Fax: +81-82-424-0725. E-mail: maida@hiroshima-u.ac.jp.

TABLE 1: Numbers of Rooted Graphs, Rooted Digraphs, and Restrictive Rooted Digraphs of PW Clusters $\text{H}_3\text{O}^+(\text{H}_2\text{O})_{n-1}$ ($n = 2$ to 7) and the Number of Stable Structures of PW Clusters $\text{H}_3\text{O}^+(\text{H}_2\text{O})_{n-1}$ ($n = 2$ to 6)

n		2	3	4	5	6	7
rooted graph		1	3	11	58	294	1806
rooted digraph		2	9	63	561	5843	68696
restrictive rooted digraph			1	5	39	338	3523
topology-distinct local minimum structures	MP2/6-31G**	1	1	3	9	43	
	MP2/aug-cc-pVDZ	1	1	3	8	30	
	B3LYP/6-31G**	1	1	3	9	31	
	B3LYP/aug-cc-pVDZ	1	1	3	5	25	

and is otherwise equal to 0. Because the HB possesses the direction and corresponding vertices, to represent the feature of the HB in the PW cluster, we use a rooted directed graph (digraph). A rooted digraph is a set of vertices and arrows. A rooted digraph has the corresponding matrix representation. For a rooted digraph with n vertices, the directed adjacency matrix, \mathbf{H} , is the n th order square matrix, whose element, h_{ij} , is equal to 1 for an arrow directed from vertex i to vertex j and is otherwise equal to 0. PW clusters can be represented by rooted digraphs, where the vertices correspond to PW or water molecules and arrows correspond to HBs from proton donor to proton acceptor. We call the representative adjacency matrix the “HB matrix.” All of the possible structures that are topology distinct can be obtained by means of the HB matrix, that is, by counting all of the possible rooted digraphs under the conditions of forming PW clusters.

The number of enumerated rooted graphs and rooted digraphs of PW clusters $\text{H}_3\text{O}^+(\text{H}_2\text{O})_{n-1}$ ($n = 2$ to 7) are given in Table 1. Various initial geometries for a PW cluster corresponding to these possible rooted digraphs (for $n = 2$ to 4) were constructed, and each of the trial geometries was optimized by means of ab initio MO method. As seen in Table 1, although the number of possible topology-distinct rooted digraphs increases rapidly with cluster size, the number of stable topology distinct structures is very limited; for example, only 1 local minimum out of 9 rooted digraphs and only 3 local minima out of 63 rooted digraphs are found for trimer and tetramer, respectively. Making use of these results as well as other previous works,^{11,13–25} we extracted the four structural rules given below and found the restrictions that a rooted digraph corresponding to a stable structures for PW clusters should fulfill. Here we call a vertex that corresponds to a protonated water molecule a P vertex and a vertex that corresponds to a water molecule a W vertex (RRDG-1: There is no arrow directed toward the P vertex; RRDG-2: The number of arrows directed from the P vertex is two or three; RRDG-3: When two arrows are directed from the P vertex, no W vertex that accepts an arrow from the P vertex can accept an arrow from another vertex; RRDG-4: When three arrows are directed from the P vertex, up to two of the W vertices, each of which accepts an arrow from the P vertex, can accept an arrow from another vertex).

We remove those HB patterns that do not fulfill these restrictions from all possible topology distinct HB patterns and generate the restrictive rooted digraphs by means of our FORTRAN program. The algorithm and the procedure for enumerating all possible and restrictive topology-distinct HB patterns of PW clusters has been described in detail elsewhere.³⁷

The corresponding HB patterns of restrictive rooted digraphs supply ideal initial structures for searching local minima of medium-sized PW clusters (i.e., $n = 5$ to 6) systematically. Any local minimum on the potential energy surface of a PW cluster must belong to one of all of the topology-distinct HB patterns. For each of the restricted HB patterns of PW clusters

$\text{H}_3\text{O}^+(\text{H}_2\text{O})_{n-1}$ ($n = 4$ to 6), we constructed various trial initial geometries by the use of a graphical tool of Mac Spartan Pro.³⁸ For each of the trial geometries, we performed the geometry optimization by means of the ab initio MO method at the MP2(full)/6-31G** and MP2(full)/aug-cc-pVDZ levels of theory^{39–42} and the DFT method at the B3LYP/6-31G** and aug-cc-pVDZ levels of theory.^{40–44} We obtained all of the optimized structures that are topologically distinguishable for each $\text{H}_3\text{O}^+(\text{H}_2\text{O})_{n-1}$ ($n = 4$ to 6). The program package Gaussian 03⁴⁹ was used for both the ab initio MO and DFT calculations as well as the harmonic vibrational frequencies and IR intensities. We confirmed that all of the optimized structures in the current work are local minima with all positive harmonic frequencies.

Results and Discussion

We have enumerated the rooted graphs, rooted digraphs and restrictive rooted digraph ($n \geq 3$) that correspond to PW clusters $\text{H}_3\text{O}^+(\text{H}_2\text{O})_{n-1}$ ($n = 2$ to 7). The numbers of the generated rooted graphs, the generated rooted digraphs, and the generated restrictive rooted digraphs and the corresponding number of local minima are summarized in Table 1. It should be noted here that we deal with only topology-distinct geometries in the current work. We do not take into account any fine structures of PW clusters, such as the direction of a free O–H bond. The optimized geometries of the PW clusters $\text{H}_3\text{O}^+(\text{H}_2\text{O})_{n-1}$ ($n = 2$ to 5) are shown in Figure S1 in the Supporting Information. The calculated IR vibrational spectra of stable structures of PW clusters (dimer, trimer, tetramer, pentamer, hexamer, and heptamer) are compared with the experimental IR spectra in Figures S2–S7, respectively, in the Supporting Information. Calculated harmonic frequencies corresponding to O–H stretching modes of PW clusters $\text{H}_3\text{O}^+(\text{H}_2\text{O})_{n-1}$ ($n = 2$ to 7) and the comparison with the experimental vibrational frequencies are summarized in Table 2. Calculated vibrational frequencies represented by different colors are given in Table 3, and the corresponding different types of hydrogen bonded O–H of the local minima of PW clusters depicted by different colors are given in Figures 2, 3, 4, 5, 7, and 9, respectively. In the current work, calculated harmonic frequencies at the MP2/aug-cc-pVDZ level of theory are scaled by 0.955, except for the proton oscillation of the Zundel core. The total energy E_{total} , the total energy with the correction of zero-point energy, E_{ZPE} , and the free energy, G (at 298.15 K), for each of the selected structures are listed in Table 4 in the order of E_{ZPE} in each cluster size. The numbering in the second column of Tables 3 and 4 corresponds to the order in G in each cluster size. In some of the cases, the order in E_{total} is different from that in E_{ZPE} , G , or both.

Protonated Water Dimer. The optimized structure (1A in Figure S1 in the Supporting Information) is in C_2 symmetry, which is the Zundel cation.^{7,11,16,17,19,29} Calculated and experimental IR spectra of PW dimer are shown in Figure S2 in the

TABLE 2: Theoretical and Experimental Vibrational Frequencies of PW Clusters $\text{H}_3\text{O}^+(\text{H}_2\text{O})_{n-1}$ ($n = 2$ to 7)^a

global minima of PW cluster		description ^b	ν_{calcd} (cm ⁻¹)			ν_{exptl} (cm ⁻¹)	
			this work	ref 11	ref 31 ^c	ref 11	ref 7
$n = 2$	<u>1A</u>	proton oscillation	798	807	774	1085	920 ^d
		H ₂ O symmetric	3552, 3559	3552, 3558	3560, 3567	3520	3609
		H ₂ O asymmetric	3661, 3661	3661, 3660	3669	3660	3684
$n = 3$	<u>2A</u>	H ₃ O ⁺ asymmetric	2387	2381		1880	
		H ₃ O ⁺ symmetric	2515	2509		2420	
		H ₂ O symmetric	3606	3604, 3605		3639	3637
		H ₃ O ⁺ free O–H	3626	3626		3580	3667
		H ₂ O asymmetric	3719	3718, 3718		3724	3722
$n = 4$	<u>3A</u>	H ₃ O ⁺ asymmetric	2806	2804	2811	2665	
		H ₃ O ⁺ symmetric	2875	2874	2880		
		H ₂ O symmetric	3613, 3614	3612, 3613	3619	3644	3645
		H ₂ O asymmetric	3725, 3726	3725, 3725	3733	3730	3730
		H ₃ O ⁺ to AD H ₂ O ^e	2347	2344		1885	
$n = 5$	<u>4A</u>	H ₃ O ⁺ asymmetric	2944	2942		2860	2879
		H ₃ O ⁺ symmetric	2970	2971			2967
		AD H ₂ O HB	3264	3257		3195	3208
		fH ₂ O symmetric	3617–3620	3615–3623		3647	3647
		AD H ₂ O fOH bond	3692	3695		3712	3736
		fH ₂ O asymmetric	3731–3737	3729–3741		3740	3817
		proton oscillation	1177	1209	1153	1055	
$n = 6$	<u>5L1</u>	H ₂ O in H ₅ O ₂ ⁺ symmetric	3125	3128	3135	3160	2988
		H ₂ O in H ₅ O ₂ ⁺ asymmetric	3138	3143	3151		3178
		H ₂ O in H ₅ O ₂ ⁺ symmetric	3277	3274	3280		
		H ₂ O in H ₅ O ₂ ⁺ asymmetric	3323	3320	3326		3320
		fH ₂ O symmetric	3619–3627	3618–3625	3626	3650	3651
		fH ₂ O asymmetric	3736–3746	3734–3744	3742	3740	3741
$n = 7$ ^f	<u>7R1</u>	proton oscillation	1291		1280	1055	
		bOH in H ₅ O ₂ ⁺ symmetric	3041, 3297		3046, 3293	3040, 3290	
		bOH in H ₅ O ₂ ⁺ asymmetric	3149, 3361		3153, 3361	3160, 3340	
		bOH in AD H ₂ O symmetric	3494, 3549		3495, 3548	3490, 3530	
		bOH in AD H ₂ O asymmetric	3724, 3736 3617,		3722, 3726 3615		
		fH ₂ O symmetric	3642, 3648 3729		3641, 3648 3733	3640, 3670	
		fH ₂ O asymmetric	3760, 3769		3759, 3768	3710, 3730	

^a Vibrational frequencies at the MP2/aug-cc-pVDZ level of theory were scaled by 0.954 to account approximately for vibrational frequency in ref 31 and 0.955 in our works as well as in ref 11. ^b fH₂O denotes free OH in H₂O, and bOH denotes hydrogen-bonded OH. ^c Calculated vibrational frequencies for heptamer are from ref 47. ^d Ref 8. ^e AD H₂O denotes the H₂O molecules that donate and accept an H bond to and from other H₂O/H₃O⁺. ^f For PW heptamer, vibrational frequencies were scaled by 0.96 in our works as well as in ref 47.

Supporting Information, and the experimental vibrational frequencies are shown in Table 2. The harmonic frequencies at the MP2(full)/aug-cc-pVDZ level of theory for asymmetric and symmetric stretchings of free O–H in PW dimer (~ 3660 and ~ 3550 cm⁻¹, respectively) compare well with the experimental values (3660 and 3520 cm⁻¹)^{7,11} and with the previous theoretical work³¹ (Table 2). The vibrational frequency at 798 cm⁻¹ (orange in Table 3) corresponds to the shared proton oscillation in O–H–O of Zundel core. As is well known, the harmonic frequency for this mode does not agree with the experimental fundamental frequency. The anharmonic treatment is mandatory, which is beyond the scope of the current work. We do not treat the inadequacy of the harmonic frequency for this mode here. Instead, we deal with PW clusters from the topological point of view, as shown in Figure 2. Each of the two water molecules that share a proton between them is called Z0 here. At the global minimum, two Z0 water molecules are symmetrically the same.

Protonated Water Trimer. The number of topology-distinct rooted digraphs with three vertices is nine, and there is only one restrictive rooted digraph. The corresponding structure of this restrictive rooted digraph is just the global minimum of PW trimer. Calculated IR spectra of the optimized structure (2A in Figure S1 in the Supporting Information) with C_s symmetry and the experimental spectra are shown in Figure S3 in the Supporting Information, and the comparison with the experimental vibrational frequencies is shown in Table 2. The schematic drawing of the PW trimer is given in Figure 3. There

are three types of O–H bonds in the PW trimer: the O–H of Eigen core, which is hydrogen bonded to two acceptor water (1A) molecules (denoted by violet arrow in Figure 3), free O–H of PW, and free O–H of A-W. A-W denotes a water molecule that accepts HB. The vibrational frequencies of symmetric and asymmetric stretches are in good agreement with the corresponding experimental values^{6,7} (Figure S3 in the Supporting Information; Tables 2 and 3).

Protonated Water Tetramer. The number of topology-distinct rooted digraphs with 4 vertices is 63, and there are 5 restrictive rooted digraphs (Table 1). We have found that three out of five correspond to the stable structures of PW tetramers; the optimized structures and the corresponding rooted digraphs of H₃O⁺(H₂O)₃ are given in Figure S1 in the Supporting Information (3A, 3B, and 3C). These structures are in accord with previous studies.^{5,11,14,19,20,23} Both of the lowest energy minimum (in E_{ZPE} or in G), 3A, and the highest energy minimum (in E_{ZPE} or in G), 3B, have an H₃O⁺ Eigen core, whereas the linear structure, 3C, has a Zundel core. The schematic drawing of PW tetramer is given in Figure 4. The pattern 3C is the one in which two O–H bonds on both sides of Zundel type PW dimer are hydrogen-bonded to two water molecules. Each of the water molecules that share a proton between them is called Z1 here. As shown in Figure 4b, although 3C does not have C_2 symmetry at the local minimum, the two Z1 water molecules are regarded to be quasi-symmetrical. Calculated IR spectra of three local minima of PW tetramer are shown in Figure S4 in

TABLE 3: IR Vibrational Frequencies of Different Types of O–H Stretching Modes of PW Clusters

n	type	Z- OH ^a of E ^b	O-H of E ^b	O-H of E ^c	O-H of Z ^d	O-H of AD-W ^e	O-H of AD-W ^f	f O-H of P ^g	f O-H of AD-W ^h	Sym metry	free O-H of W ⁱ asymmetric	free O-H of W ⁱ symmetric
2	2-1	<u>1A</u>	798					3552, 3559 3661(2)		C2		
3	3-1	<u>2A</u>		2387 2515				3626		Cs	3719(2)	3606(2)
	4-1	<u>3A</u>		2806(2) 2875						C3	3725(3)	3613(3)
4	4-2	<u>3C</u>	1040		2925,3024			3653, 3664		C1	3727, 3729	3614, 3615
	4-3	<u>3B</u>	2260 2450			3446, 3470		3610	3682, 3686	C1	3691	3584
	5-2	<u>5A</u>	2696 2785	2911		3470 3491		3695 3699		C1	3735, 3699	3619, 3591
	5-1	<u>4A</u>	2347	2944 2970		3264		3691		C1	3737, 3731, 3730	3620, 3617(2)
5	5-4	<u>5B</u>	2023	2901 3144		3261	3607	3676, 3732		C1	3726, 3697	3613, 3586
	5-3	<u>4B</u>	2032 2236			3216 3223		3654	3699(2)	Cs	3742(2)	3624(2)
	5-5	<u>6C</u>	2585 2707	3119		3570	3530, 3534	3701, 3704		C1	3726	3586
	6-1	<u>5L1</u>	1232		3125,3138 3277,3323					C1	3619(2), 3621, 3627	3736(2) 3738,3746
	6-5	<u>6R1</u>	2608 2727	2960		3279	3359, 3407	3666,3694 3697		C1	3737, 3740	3621, 3623
	6-4	<u>6R2</u>	2222 2884	3017		3314, 3378 3551		3702		C1	3745,3739, 3706	3626,3722 3597
6	6-3	<u>6R3</u>	2486 2842 2927			3318 3485, 3504		3703,3705 3706		C1	3746, 3706	3627, 3597
	6-2	<u>5L2</u>	2504 2614	3036		3305, 3299		3700, 3697		C1	3745,3740 3734	3626,3622 3618
	6-6	<u>6R6</u>	2449 2785	3001		3441, 3530	3286	3700,3693 3708		C1	3736, 3704	3619, 3595
	7-6	<u>9C1</u>	2669 2731 2846				3411, 3425 3436, 3453 3498, 3503	3678,3679 3682,3700 3701,3709		C1		
	7-3	<u>7R1</u>	1345		3025,3132 3279,3343	3476, 3531		3704, 3717		C1	3709,3741, 3749	3598,3623 3629
	7-4	<u>7R2</u>	2558 2755 2861			3285, 3317	3377, 3422	3674,3697 3700, 3707		C1	3744, 3747	3625, 3627
7	7-5	<u>7R3</u>	2493 2630	3017			3265, 3277, 3323, 3446, 3559	3677,3687 3691,3693 3729		C1	3739	3622
	7-2	<u>6L1</u>	2657 2658 2782			3337 3330(2)		3702(3)		C1	3746(3)	3627(3)
	7-1	<u>6L2</u>	2062 2770	3133		3341,3344 3403		3705		C1	3749,3747 3740, 3738	3629,3628 3622,3621

^a Shared proton oscillation in Zundel core. ^b Stretch of OH that is hydrogen bonded from Eigen core to one acceptor, one donor water (AD-W) molecule. ^c Stretch of OH that is hydrogen bonded from Eigen core to one acceptor water (A-W) molecule. ^d Stretch of OH that is hydrogen bonded from Zundel core to A-W or AD-W molecule. ^e Stretch of OH that is hydrogen bonded from AD-W to A-W. ^f Stretch of OH that is hydrogen bonded from AD-W to AD-W. ^g Free OH stretch of PW. ^h Free OH stretch of AD-W. ⁱ Free OH stretch of A-W.

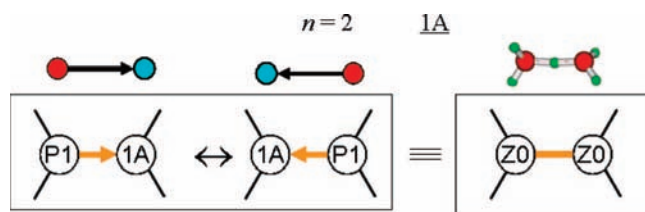


Figure 2. Schematic drawing of PW dimer. The orange arrow denotes the shared proton oscillation in O–H–O. P1 denotes a protonated water that donates one HB; 1A denotes a water molecule that accepts one HB. Because of the symmetry, a hydrogen bonding pattern in which one orange arrow directs from P1 toward 1A is equal to that with the orange arrow where P1 and 1A are exchanged. Z0 denotes a Zundel-type water molecule with no other water molecules attached.

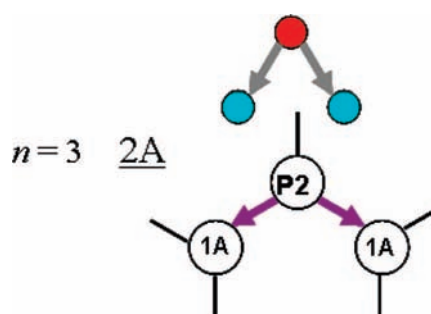


Figure 3. Schematic drawing of PW trimer. The hydrogen-bonded O–H from P2 (or H₃O⁺) to two acceptor water (1A) molecules are shown with violet arrows. P2 denotes a protonated water that donates two HBs.

the Supporting Information; calculated vibrational frequencies of the O–H stretching modes are given in Table 3, with the same coloring as that in Figure 4. Scaled harmonic frequencies of asymmetric and symmetric stretches of different types of

O–H of the global minimum 3A agree reasonably well with the previous theoretical work³¹ and experimental results^{5,7,11} (Figure S4 in the Supporting Information and Table 2).

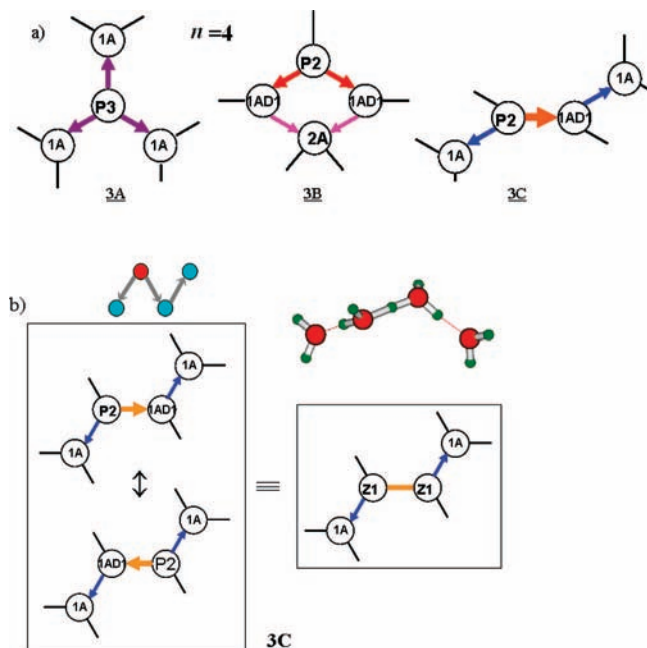


Figure 4. Schematic drawing of PW tetramer. (a) Violet arrows denote hydrogen-bonded OHs of P3 to three 1A water molecules in 3A. Red arrows denote hydrogen-bonded OHs of P2 to 1AD1 water molecules (which accept one HB and donate one HB). Pink arrows denote hydrogen-bonded OHs of 1AD1 water to 2A water (which accepts two HBs) in 3B. An orange arrow denotes Zundel OH, and blue arrows denote hydrogen-bonded OH of Zundel core to 1A in 3C. (b) Schematic drawing of PW tetramer 3C with the rooted digraph and the optimized geometry. A hydrogen bonding pattern in which one orange arrow directs from P2 toward 1AD1 is almost equal to that with the reversed orange arrow where P2 and 1AD1 are exchanged. Z1 denotes a Zundel-type water molecule with one water molecule hydrogen bonded.

Protonated Water Pentamer. Among 561 possible rooted digraphs, 39 restrictive rooted digraphs were generated for PW pentamers, and various initial geometries were constructed for a PW pentamer with an HB topology corresponding to each of the above restrictive rooted digraphs, followed by the geometry optimization by means of the *ab initio* MO method and DFT method with various basis sets. We found 9 local minima out of 39 restrictive rooted digraphs by means of both MP2(full)/6-31G** and B3LYP/6-31G** and 8 and 5 out of 39 with MP2(full)/aug-cc-pVDZ and B3LYP/aug-cc-pVDZ levels of theory, respectively (Table 1). The optimized structures with MP2(full)/aug-cc-pVDZ and the corresponding rooted digraphs of eight local minima of PW pentamers are given Figure S1 in the Supporting Information. All of the local minima of PW pentamers are in C_1 symmetry except 4B. IR spectra of the five

lowest E_{ZPE} minima of $H_3O^+(H_2O)_4$ are shown Figure S5 in the Supporting Information. The O–H bonds in PW pentamers are classified and denoted by arrows/lines with different colors in Figure 5. The corresponding vibrational frequencies are listed in Table 3.

According to E_{total} and also according to E_{ZPE} , the pattern 5A is the lowest energy minimum of PW pentamers; Hodges and Wales,¹⁶ Christie and Jordan,²⁰ Mella,²³ Kuo,²⁷ and Corongiu²⁶ also reported 5A as the global minimum by means of Monte Carlo simulation with ASP potential method,¹⁶ MSEVB potential method,^{20,50} OSS2,²⁷ OSS3 potential method,²³ and MMCP and DFT calculation,²⁶ respectively. The pattern 4A is lower in free energy than 5A by $1.89 \text{ kcal}\cdot\text{mol}^{-1}$ at 298.15 K (Table 4). The experimental OH vibrational frequencies¹¹ can be explained on the basis of the calculated frequencies of 4A with a possible coexistence of 5A (Figure S5 in the Supporting Information and Table 2). We note that the conversion between 5A and 4A can easily proceed only by the formation/dissociation of one HB. It is probable that the relative ratio between the clusters depends on the experimental condition.

Both PW pentamer 5A (Figure 5) and PW tetramer 3B (Figure 4) include a four-member ring structure. 5A of PW pentamer can be regarded as being formed by attaching one water molecule to free O–H of Eigen core in 3B PW tetramer. The O–H stretching frequencies in red (Table 3) are blue-shifted after the one water attachment, which indicates that the corresponding O–H bonds are stronger and the corresponding HBs are weaker in 5A than in 3B.

PW pentamer 4B (Figure 5) has a H_3O^+ Eigen core and is a unique pattern with C_s symmetry, in which two water molecules are hydrogen-bonded to two free O–H bonds on two dangling water molecules of Eigen-type PW trimer 2A (Figure 2). The stretching frequencies of the two O–H bonds (red arrows) of PW in 4B, each of which is hydrogen bonded to a neighbor water molecule, are lower than those of the corresponding two O–H bonds (violet arrows) of PW in 2A, which indicates that the O–H bonds of PW are weaker in PW pentamer 4B than those in PW trimer 2A (Table 3) and the corresponding HBs are stronger in 4B than in 2A. The strongest HB in PW pentamer corresponds to the red arrow in 5B, followed by those in 4B, because the O–H stretching frequencies for those O–H bonds are highly red shifted (O–H of E column in Table 3).

Protonated Water Hexamer. Among 5843 possible rooted digraphs, 338 restrictive rooted digraphs were generated for PW cluster hexamer, and various initial geometries were constructed for a PW hexamer with an HB topology corresponding to each of the above restrictive rooted digraphs, followed by the geometry optimization by means of the *ab initio* MO method and DFT method with various basis sets. We found 43, 30, 31,

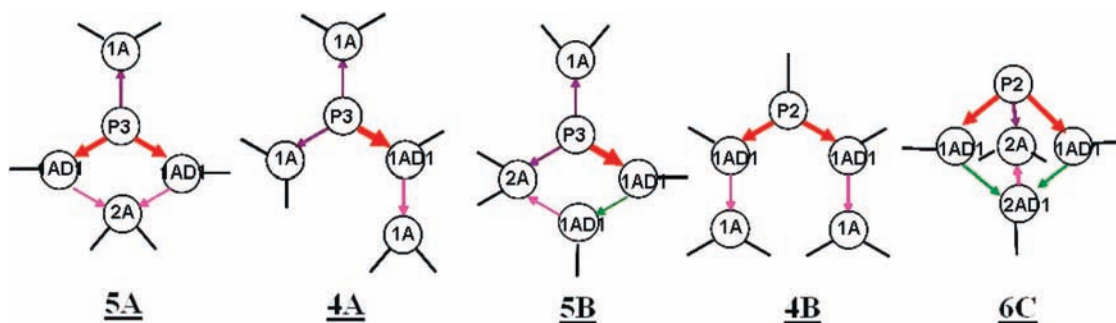


Figure 5. Schematic drawing of PW pentamers. Red arrow denotes O–H of PW that is hydrogen bonded to AD-W (which accepts HB and donates HB). Violet arrow denotes O–H of PW that is hydrogen bonded to A-W (which accepts HB). Pink arrow denotes O–H of AD-W that is hydrogen bonded to A-W. Black lines indicate free O–H bonds of PW, AD-W, and A-W.

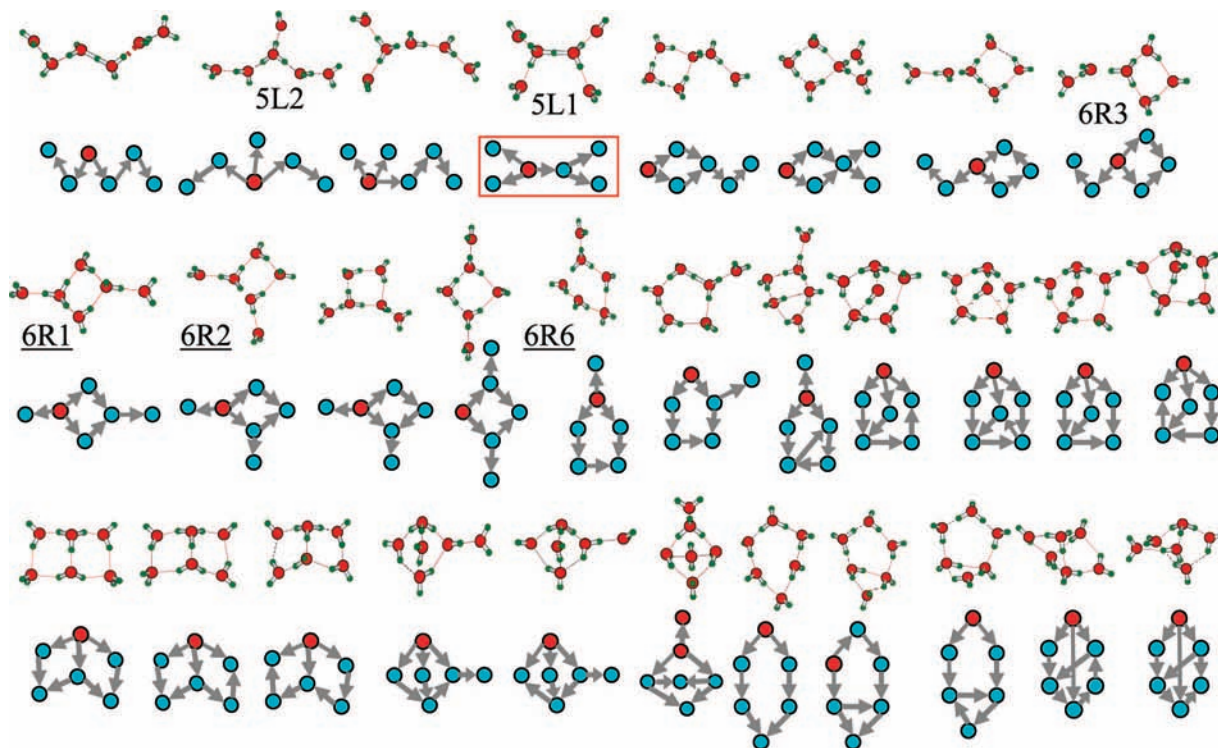


Figure 6. Rooted digraphs and optimized structures of PW hexamers $\text{H}_3\text{O}^+(\text{H}_2\text{O})_5$ (MP2/aug-cc-pVDZ). The designated patterns (5L1, 5L2, 6R1, 6R2, 6R3, and 6R6) correspond to the six lowest energy minimum structures.

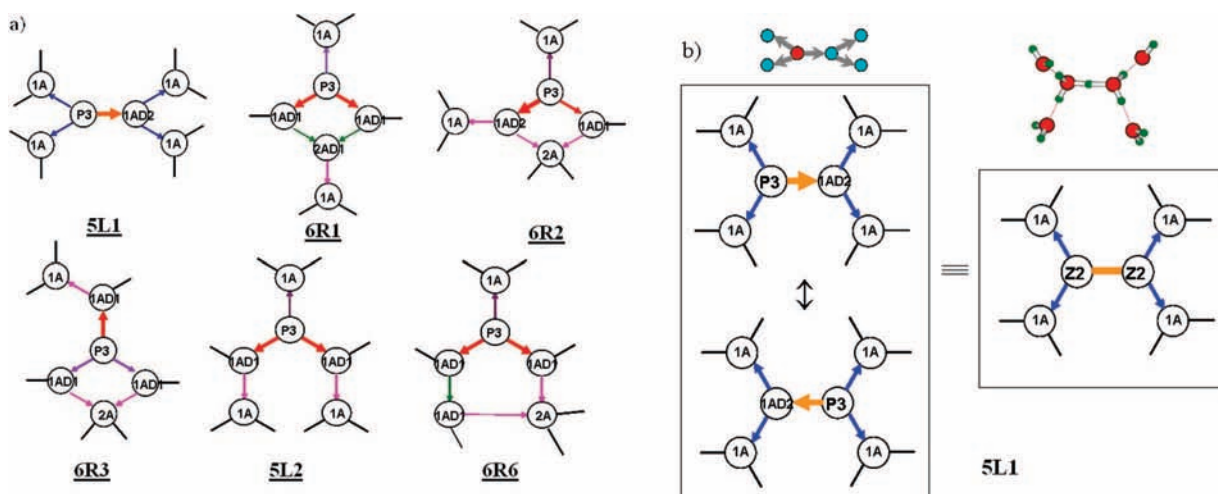


Figure 7. Schematic drawing of PW hexamers. (a) Six lowest energy minimum (in E_{ZPE}) PW clusters, 5L1, 6R1, 6R2, 6R3, 5L2, and 6R6. (b) Schematic drawing of PW hexamer 5L1 with the rooted digraph and the optimized geometry. A hydrogen bonding pattern in which one orange arrow directs from P3 toward 1AD2 can be regarded to be almost equal to the one with the reversed orange arrow where P3 and 1AD2 are exchanged. Z2 denotes a Zundel-type water molecule with two water molecules hydrogen bonded.

and 25 local minima out of 338 restrictive rooted digraphs at MP2(full)/6-31G**, MP2(full)/aug-cc-pVDZ, B3LYP/6-31G**, and B3LYP/aug-cc-pVDZ levels of theory, respectively (Table 1).

The optimized geometries that are obtained with MP2(full)/aug-cc-pVDZ and those corresponding restrictive rooted digraphs are shown in Figure 6. Many new local minima with seven and eight HBs that had not been reported in previous works^{5,21,27,28,50} were found. All of the obtained local minima of hexamers are of C_1 symmetry. As seen in Table 4, 6R1 is the lowest in E_{total} (i.e., at the bottom of potential energy surface) of PW hexamers, whereas 5L1 is the lowest in E_{ZPE} (with zero point energy correction). It is probable that the most free-energetically stable structure may depend on the experimental condition. In our calculation, 5L1 is the most stable in both

E_{ZPE} and in G , which is topologically the same as that found by means of Monte Carlo method with MSEVB potential methods,²¹ ab initio MP2 method, and DFT method.^{5,28} That is different, however, from the one found from Monte Carlo with the basin-hopping algorithm with KJ and ASP potential method,¹⁶ OSS2/OSS3 potential method,^{24,27} and MSEVB4P method.⁵⁰

IR spectra and vibrational frequencies with MP2(full)/aug-cc-pVDZ level of theory of the six lowest energy minima in E_{ZPE} (5L1, 6R1, 6R2, 6R3, 5L2, and 6R6 in Figure 6) of PW hexamers $\text{H}_3\text{O}^+(\text{H}_2\text{O})_5$ are shown in Figure S6 in the Supporting Information and Table 3. Schematic drawings of those six hexamers are shown in Figure 7a.

The free-energetically, most stable PW hexamer, 5L1, has Zundel character, as shown in Figure 7b. Each of the two water

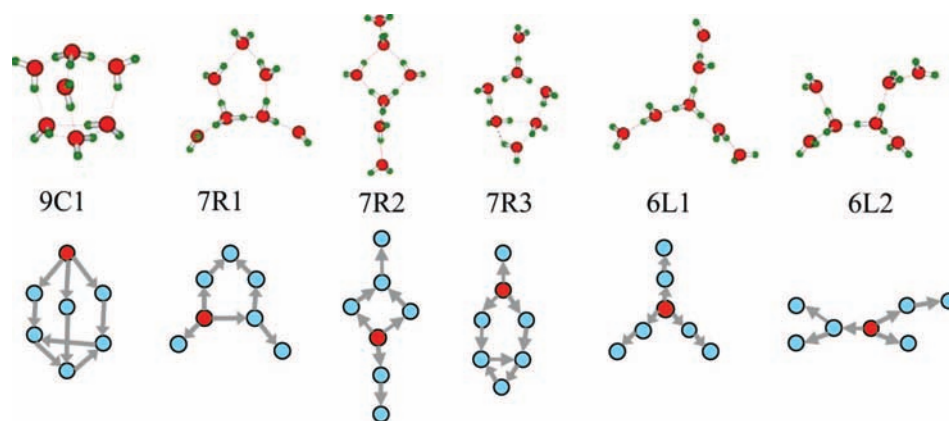


Figure 8. Restrictive rooted digraphs and optimized structures of six lower energy minima (in E_{ZPE}) of PW heptamers $\text{H}_3\text{O}^+(\text{H}_2\text{O})_6$.

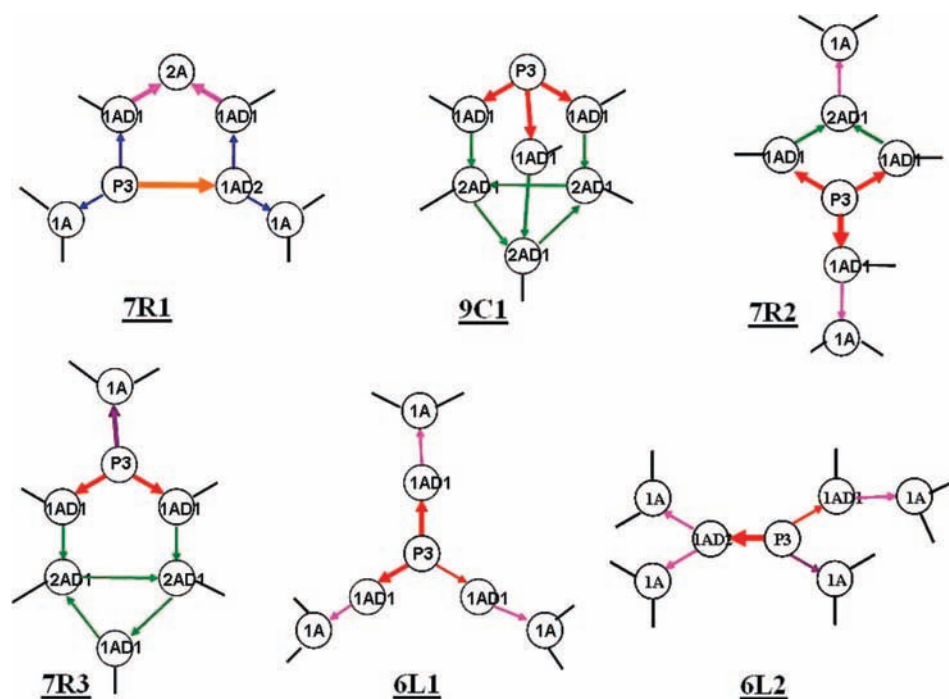


Figure 9. Schematic drawing of six lower energy minima (in E_{ZPE}) of the PW heptamer.

molecules that share a proton between them is called Z2 here. Although 5L1 does not have C_2 symmetry at the local minimum, two Z2 water molecules are regarded to be quasi-symmetrical.

Four-member ring minima, 6R1, 6R2, and 6R3, are 0.39, 0.42, and 0.46 $\text{kcal}\cdot\text{mol}^{-1}$ higher in E_{ZPE} than is 5L1 (Table 4), respectively. Each of these is formed by attaching one water molecule to a free O–H in PW pentamer 5A. The difference in the attaching position creates different O–H classifications, resulting in different O–H stretching frequencies (Table 3). The differently classified O–H bonds are colored differently in Figure 7a. Among the red-colored O–H stretching modes in ring hexamers, 6R2 possesses the lowest frequency mode, which originated from hydrogen bonding between PW and 1AD2 water molecules. The 1AD2 water molecule is the one that accepts one HB from PW and donates two HBs, resulting in a stronger hydrogen bond between PW and 1AD2.

Protonated Water Heptamer. As the cluster increases in size, the number of local minima explosively increases; furthermore, their energy differences diminish with n .⁴⁴ Among 68 696 possible rooted digraphs, 3523 restrictive rooted digraphs were generated for PW cluster heptamer, and various initial geometries were constructed for a PW heptamer with an HB

topology corresponding to each of the above restrictive rooted digraphs, followed by the geometry optimization by means of MP2(full)/aug-cc-pVDZ level of theory. We found a large number of local minima. The optimized structures, corresponding rooted digraphs, and optimized structures of six lower energy minima (in E_{ZPE}) of the PW heptamer $\text{H}_3\text{O}^+(\text{H}_2\text{O})_6$ with MP2(full)/aug-cc-pVDZ level of theory are shown in Figure 8; these are denoted by 7R1, 9C1, 7R2, 7R3, 6L1, and 6L2. The calculated IR spectra and their vibrational frequencies with MP2(full)/aug-cc-pVDZ level of theory are shown in Figure S7 in the Supporting Information and Table 3. All of six local minima of the PW heptamers are of C_1 symmetry.

According to E_{total} and also according to E_{ZPE} , the pattern 9C1 is the lowest energy minimum of PW heptamers; also, some previous theoretical works^{15,16,27} reported this pattern to be the global minimum. Free energy calculation at 298.15 K shows that 9C1 is not the most stable (Table 4); there are various other structures that have similar free energies including 7R1, 6L1, and 6L2. Therefore the most stable structure may depend on the temperature or experimental conditions. The pattern 7R1 is topologically the same as the one found by means of DFT

TABLE 4: Total Energy (E_{total}), Total Energy with Zero Point Energy Correction (E_{ZPE}), and Free Energy (G) at 298.15 K of PW Clusters $\text{H}_3\text{O}^+(\text{H}_2\text{O})_{n-1}$ ($n = 2$ to 7) (MP2/aug-cc-pVDZ)

n	type	E_{total} (E_{h})	E_{ZPE} (E_{h})	G (E_{h})	ΔE_{total} (kcal mol $^{-1}$)	ΔE_{ZPE} (kcal mol $^{-1}$)	ΔG (kcal mol $^{-1}$)
2	2-1 <u>1A</u> (Zundel)	-152.850505	-152.793815	-152.818519		0	
3	3-1 <u>2A</u> (Eigen)	-229.152027	-229.068644	-229.099173		0	
4	4-1 <u>3A</u> (Eigen)	-305.447469	-305.338913	-305.373930	0	0	0
	4-2 <u>3C</u> (Zundel)	-305.441202	-305.335167	-305.371633	3.93	2.35	1.44
5	4-3 <u>3B</u> (Eigen)	-305.441518	-305.331511	-305.364483	3.73	4.64	5.93
	5-2 <u>5A</u> (Eigen)	-381.734809	-381.599947	-381.638678	0	0	0
	5-1 <u>4A</u> (Eigen)	-381.732953	-381.599888	-381.641695	1.16	0.04	-1.89
	5-4 <u>5B</u> (Eigen)	-381.730835	-381.597016	-381.636542	2.49	1.84	1.34
	5-3 <u>4B</u> (Eigen)	-381.726832	-381.595363	-381.638097	5.01	2.88	0.36
6	5-5 <u>6C</u> (Eigen)	-381.730131	-381.594411	-381.631629	2.94	3.47	4.42
	6-1 <u>5L1</u> (Zundel)	-458.015907	-457.860556	-457.908853	0	0	0
	6-5 <u>6R1</u> (Eigen)	-458.019402	-457.859937	-457.904487	-2.19	0.39	2.74
	6-4 <u>6R2</u> (Eigen)	-458.018520	-457.859889	-457.904776	-1.64	0.42	2.56
	6-3 <u>6R3</u> (Eigen)	-458.018861	-457.859822	-457.905134	-1.85	0.46	2.33
	6-2 <u>5L2</u> (Eigen)	-458.016970	-457.859432	-457.907450	-0.67	0.71	0.88
	6-6 <u>6R6</u> (Eigen)	-458.018723	-457.859100	-457.902794	-1.77	0.92	3.80
7	7-6 <u>9C1</u> (Eigen)	-534.306877	-534.119870	-534.163557	0	0	0
	7-3 <u>7R1</u> (Zundel)	-534.301260	-534.119790	-534.171268	3.52	0.05	-4.84
	7-4 <u>7R2</u> (Eigen)	-534.302848	-534.119070	-534.169853	2.53	0.51	-3.95
	7-5 <u>7R3</u> (Eigen)	-534.303093	-534.117980	-534.165593	2.37	1.19	-1.28
	7-2 <u>6L1</u> (Eigen)	-534.299563	-534.117720	-534.172348	4.59	1.35	-5.52
	7-1 <u>6L2</u> (Eigen)	-534.298238	-534.117450	-534.172352	5.42	1.52	-5.52

method,⁵ ab initio MP2 method,¹¹ CPMD simulation methods,⁴⁷ and DFT and ab initio MP2 methods.^{46,48}

The pattern 7R1 can be regarded to be formed by attaching one H_2O to the center of the two free O–H bonds of two A–W molecules in Zundel-like minimum 5L1 of PW hexamer (Figures 6 and 7). The attachment of one water molecule does not largely affect the O–H stretching frequencies (Table 3). Therefore, the shared proton oscillation frequency (orange colored) is only slightly higher in 7R1 than in 5L1; the blue-colored O–H stretching modes in 7R1 are similar to those in 5L1, which are hydrogen bonded from the Zundel core to A–W or AD–W molecules.

The pattern 7R3 can be regarded to be formed by attaching one H_2O to a local minimum 6R6 of PW hexamer (Figures 6 and 7). This attachment does not change the O–H frequencies of the corresponding O–H bonds in those clusters, although the pink-colored OH type (~ 3500 cm^{-1}) disappears in 7R3.

OH Types in Protonated Water Cluster. The following is the summary of the O–H stretching modes found in PW clusters $\text{H}_3\text{O}^+(\text{H}_2\text{O})_{n-1}$ ($n = 2$ to 7). We find that the O–H bonds in PW clusters are divided into the nine types: (1) The Zundel-type OH, which is in each of the Zundel-type stable structures, that is, the global minimum 1A of PW dimer and the local minimum 3C of PW tetramer and the lowest energy minimum (in E_{ZPE} and in G) 5L1 of PW hexamer and the local minimum 7R1 of PW heptamer, represented in orange in Table 3 and Figures 2, 4, 7, and 9. Only the PW dimer 1A is of C_2 symmetry, whereas the other Zundel-type PW clusters are of C_1 symmetry. The order of the shared proton oscillation frequencies is 1A < 3C < 5L1 < 7R1 (shown in orange in Table 3), indicating that the order of the proton-sharing character in Zundel-type PW clusters is $Z0 > Z1 > Z2$. (2) The OH bonds of Eigen-type PW, which are hydrogen bonded to AD–W, represented in red in Table 3 and Figures 4, 5, 7, and 9. This type is included in all of the Eigen-type PW tetramers and larger PW clusters. The distribution of the frequency of this type is very wide, covering ~ 2000 to ~ 2900 cm^{-1} . (3) The OH bonds of Eigen-type PW, which are hydrogen-bonded to A–W, represented in violet in Table 3 and Figures 3, 4, 5, 7 and 9. The distribution of the frequency of this type is rather wide, covering ~ 2300 to ~ 3100

cm^{-1} . (4) The OH bonds of Zundel-type PW, which are hydrogen bonded to A–W or AD–W, represented in blue in Table 3 and Figures 4, 7, and 9. The distribution of the frequency of this type is rather narrow, covering ~ 2900 to ~ 3300 cm^{-1} . (5) The OH bonds of AD–W, which are hydrogen-bonded to A–W, represented in pink in Table 3 and Figures 4, 5, 7, and 9. The distribution of the frequency of this type is rather narrow, covering ~ 3200 to ~ 3500 cm^{-1} . (6) The OH bonds of AD–W, which are hydrogen bonded to AD–W, represented in green in Table 3 and Figures 5, 7, and 9. The distribution of the frequency of this type is rather narrow, covering ~ 3300 to ~ 3600 cm^{-1} . (7) Free OH bonds of PW that are not hydrogen bonded. (8) Free OH bonds of AD–W, which are not hydrogen bonded. (9) Free OH bonds of A–W, which are not hydrogen bonded.

The O–H stretching frequencies in PW clusters distribute very widely. The O–H stretching frequencies increase in order from type 1 to type 9, as summarized in Table 3. The lowest frequency around 1000 cm^{-1} corresponds to the shared proton oscillation in Zundel-type PW clusters. The modes in the range from ~ 2000 to ~ 3000 cm^{-1} correspond to O–H stretching of PW in Eigen-type PW clusters. It is noteworthy that there is no mode in this region for Zundel-type PW clusters. The highest frequency around 3700 cm^{-1} corresponds to a stretching mode of free O–H of A–W in PW clusters. The lowest frequency of O–H stretching of neutral water molecules in PW clusters is around ~ 3200 cm^{-1} , which corresponds to the O–H stretching mode of AD–W, which accepts HB from PW and donates HB to A–W or to AD–W. The hydrogen bonding is strong in such cases, and the HB strength depends on HB pattern.

Conclusions

We showed here the systematical method to find all possible structures of PW clusters. We extracted the restrictions that a stable structure of a PW cluster should fulfill. The enumeration method in the frame of graph theory together with the extraction of the restrictions can be used to obtain all possible hydrogen bonding patterns corresponding to PW clusters. By combining the graph theoretical enumeration with ab initio MO calculations, we found all topology-distinct stable structures of PW clusters

up to hexamer. Although the numbers and the structures of stable PW clusters may vary depending on the MO method used, the graph theoretical enumeration method guarantees that there cannot be any other patterns.

We classified all of the O–H bonds in PW clusters up to heptamer into nine types according to the difference in the hydrogen bonding patterns: each type is accompanied by a specific range of stretching frequency. The distinction between Zundel-type and Eigen-type PW clusters can be achieved on the basis of the calculated stretching frequencies at the MP2/aug-cc-pVDZ level of theory. Experimental IR spectra are well characterized on the basis of the calculated O–H stretching frequencies of stable PW clusters.

Acknowledgment. The calculations were carried out in part at the Research Center for Computational Science, Okazaki National Research Institutes. This study was partially supported by grants from the Ministry of Education, Culture, Sports, Science and Technology of Japan.

Supporting Information Available: Optimized geometries, calculated IR vibrational spectra of stable structures of PW clusters (dimer, trimer, tetramer, pentamer, hexamer, and heptamer) and comparisons with the experimental IR spectra. This material is available free of charge via the Internet at <http://pubs.acs.org>.

References and Notes

- (1) Ferguson, E. E.; Arnold, F. *Acc. Chem. Res.* **1981**, *14*, 327.
- (2) Wayne, R. P. *Chemistry of Atmospheres*; Oxford University Press: Oxford, U.K., 1991.
- (3) Seinfeld, J. H.; Pandis, S. N. *Atmospheric Chemistry and Physics: From Air Pollution to Climate Change*; Wiley: New York, 1997.
- (4) Baciou, L.; Michel, H. *Biochemistry* **1995**, *34*, 7967.
- (5) Jiang, J.-C.; Wang, Y.-S.; Chang, H.-C.; Lin, S. H.; Lee, Y. T.; Schatteburg, G. N.; Chang, H.-C. *J. Am. Chem. Soc.* **2000**, *122*, 1398.
- (6) Okumura, M.; Yeh, L. I.; Myers, J. D.; Lee, Y. T. *J. Chem. Phys.* **1986**, *85*, 2328.
- (7) Yeh, L. I.; Okumura, M.; Myers, J. D.; Price, J. M.; Lee, Y. T. *J. Chem. Phys.* **1989**, *91*, 7319.
- (8) Asmis, K. R.; Pivonka, N. L.; Santambrogio, G.; Brümmer, M.; Kaposta, C.; Neumark, D. M.; Wöste, L. *Science* **2003**, *299*, 1375.
- (9) Miyazaki, M.; Fujii, A.; Ebata, T.; Mikami, N. *Science* **2004**, *304*, 1134.
- (10) Shin, J. W.; Hammer, N. I.; Diken, E. G.; Johnson, M. A.; Walters, R. S.; Jaeger, T. D.; Duncan, M. A.; Christie, R. A.; Jordan, K. D. *Science* **2004**, *304*, 1137.
- (11) Headrick, J. M.; Diken, E. G.; Walters, R. S.; Hammer, N. I.; Christie, R. A.; Cui, J.; Myshakin, E. M.; Duncan, M. A.; Johnson, M. A.; Jordan, K. D. *Science* **2005**, *308*, 1765.
- (12) Xie, Y.; Remington, R. B.; Schaefer, H. F., III. *J. Chem. Phys.* **1994**, *101*, 4878.
- (13) Wei, D.; Salahub, D. R. *J. Chem. Phys.* **1994**, *101*, 7633.
- (14) Hodges, M. P.; Stone, A. J. *J. Chem. Phys.* **1999**, *110*, 6766.
- (15) Wei, D.; Salahub, D. R. *J. Chem. Phys.* **1997**, *106*, 6086.
- (16) Hodges, M. P.; Wales, D. J. *Chem. Phys. Lett.* **2000**, *324*, 279.
- (17) Valeev, E. F.; Schaefer III, H. F. *J. Chem. Phys.* **1998**, *108*, 7197.
- (18) Wales, D. J. *J. Chem. Phys.* **1999**, *110*, 10403.
- (19) Ojamaä, L.; Shavitt, I.; Singer, S. J. *J. Chem. Phys.* **1998**, *109*, 5547.
- (20) Christie, R. A.; Jordan, K. D. *J. Phys. Chem. A* **2001**, *105*, 7551.
- (21) Christie, R. A.; Jordan, K. D. *J. Phys. Chem. B* **2002**, *106*, 8376.
- (22) Kozack, R. E.; Jordan, P. C. *J. Chem. Phys.* **1992**, *96*, 3131.
- (23) Mella, M.; Clary, D. C. *J. Chem. Phys.* **2003**, *119*, 10048.
- (24) Mella, M.; Kuo, J.-L.; Clary, D. C.; Klein, M. L. *Phys. Chem. Chem. Phys.* **2005**, *7*, 2324.
- (25) Wales, D. J. *J. Chem. Phys.* **1999**, *111*, 8429.
- (26) Corongiu, G.; Kelterbaum, R.; Kochanski, E. *J. Phys. Chem.* **1995**, *99*, 8038.
- (27) Kuo, J.-L.; Klein, M. L. *J. Chem. Phys.* **2005**, *122*, 024516.
- (28) Kuo, J.-L. *J. Phys.: Conf. Ser.* **2006**, *28*, 87.
- (29) James, T.; Wales, D. J. *J. Chem. Phys.* **2005**, *122*, 134306.
- (30) Iyengar, S. S.; Petersen, M. K.; Day, T. J. F.; Burnham, C. J.; Teige, V. E.; Voth, G. A. *J. Chem. Phys.* **2005**, *123*, 084309.
- (31) Park, M.; Shin, I.; Singh, N. J.; Kim, K. S. *J. Phys. Chem. A* **2007**, *111*, 10692.
- (32) Hosoya, H.; Gotoh, M.; Murakami, M.; Ikeda, S. *J. Chem. Inf. Comput. Sci.* **1999**, *39*, 192.
- (33) Gutman, I.; Soldatovič, T.; Vidovič, D. *Chem. Phys. Lett.* **1998**, *297*, 428.
- (34) McDonald, S.; Ojamaä, L.; Singer, S. J. *J. Phys. Chem. A* **1998**, *102*, 2824.
- (35) Miyake, T.; Aida, M. *Chem. Phys. Lett.* **2002**, *363*, 106.
- (36) Miyake, T.; Aida, M. *Internet Electron. J. Mol. Des.* **2003**, *2*, 24.
- (37) Jieli, M.; Miyake, T.; Aida, M. *Bull. Chem. Soc. Jpn.* **2007**, *80*, 2131.
- (38) *Mac Spartan Pro*; Wavefunction, Inc.: Irvine, CA, 2000.
- (39) Möller, C.; Plesset, M. S. *Phys. Rev.* **1934**, *46*, 618.
- (40) Hehre, W. J.; Ditchfield, R.; Pople, J. A. *J. Chem. Phys.* **1972**, *56*, 2257.
- (41) Hariharan, P. C.; Pople, J. A. *Theor. Chim. Acta* **1973**, *28*, 213.
- (42) Dunning, T. H., Jr. *J. Chem. Phys.* **1989**, *90*, 1007.
- (43) Parr, R. G.; Yang, W. *Density-Functional Theory of Atoms and Molecules*; Oxford University Press: Oxford, U.K., 1989.
- (44) Becke, A. D. *J. Chem. Phys.* **1993**, *98*, 5648.
- (45) Berry, R. S. *Chem. Rev.* **1993**, *93*, 2379.
- (46) Lee, H. M.; Tarakeshwar, P.; Park, J. W.; Kolaski, M. R.; Yoon, Y. J.; Yi, H.-B.; Kim, W. Y.; Kim, K. S. *J. Phys. Chem. A* **2004**, *108*, 2949.
- (47) Shin, I.; Park, M.; Min, S. K.; Lee, E. C.; Suh, S. B.; Kim, K. S. *J. Chem. Phys.* **2006**, *125*, 234305.
- (48) Singh, N. J.; Olleta, A. C.; Kumar, A.; Park, M.; Yi, H.-B.; Bandyopadhyay, I.; Lee, H. M.; Tarakeshwar, P.; Kim, K. S. *Theor. Chem. Acc.* **2006**, *115*, 127.
- (49) Frisch, M. J.; Trucks, G. W.; Schlegel, H. B.; Scuseria, G. E.; Robb, M. A.; Cheeseman, J. R.; Montgomery, J. A., Jr.; Vreven, T.; Kudin, K. N.; Burant, J. C.; Millam, J. M.; Iyengar, S. S.; Tomasi, J.; Barone, V.; Mennucci, B.; Cossi, M.; Scalmani, G.; Rega, N.; Petersson, G. A.; Nakatsuji, H.; Hada, M.; Ehara, M.; Toyota, K.; Fukuda, R.; Hasegawa, J.; Ishida, M.; Nakajima, T.; Honda, Y.; Kitao, O.; Nakai, H.; Klene, M.; Li, X.; Knox, J. E.; Hratchian, H. P.; Cross, J. B.; Bakken, V.; Adamo, C.; Jaramillo, J.; Gomperts, R.; Stratmann, R. E.; Yazyev, O.; Austin, A. J.; Cammi, R.; Pomelli, C.; Ochterski, J. W.; Ayala, P. Y.; Morokuma, K.; Voth, G. A.; Salvador, P.; Dannenberg, J. J.; Zakrzewski, V. G.; Dapprich, S.; Daniels, A. D.; Strain, M. C.; Farkas, O.; Malick, D. K.; Rabuck, A. D.; Raghavachari, K.; Foresman, J. B.; Ortiz, J. V.; Cui, Q.; Baboul, A. G.; Clifford, S.; Cioslowski, J.; Stefanov, B. B.; Liu, G.; Liashenko, A.; Piskorz, P.; Komaromi, I.; Martin, R. L.; Fox, D. J.; Keith, T.; Al-Laham, M. A.; Peng, C. Y.; Nanayakkara, A.; Challacombe, M.; Gill, P. M. W.; Johnson, B.; Chen, W.; Wong, M. W.; Gonzalez, C.; Pople, J. A. *Gaussian 03*, revision C.02; Gaussian, Inc.: Wallingford, CT, 2004.
- (50) Kumar, R.; Christie, R. A.; Jordan, K. D. *J. Phys. Chem. B*, published online Nov 12, <http://dx.doi.org/10.1021/jp8066475>.
- (51) Parthasarathi, R.; Subramanian, V.; Sathyamurthy, N. *J. Phys. Chem. A* **2007**, *111*, 13287.
- (52) Yu, H.; Cui, Q. *J. Chem. Phys.* **2007**, *127*, 234504.
- (53) Buch, V.; Dubrovskiy, A.; Mohamed, F.; Parrinello, M.; Sadlej, J.; Hammerich, A. D.; Devlin, J. P. *J. Phys. Chem. A* **2008**, *112*, 2144.

JP810735M